JMEPEG (2006) 15:608-613
DOI: 10.1361/105994906X136160

1059-9495/$19.00

Modeling of Stress Ratio Effect on Al Alloy SAE AMS 7475-T7351: Influence of Loading Direction

E. Di Todaro, C.T.O.F. Ruckert, M.T. Milan, W.W. Bose Filho, J.R. Tarpani, and D. Spinelli

(Submitted November 30, 2005; in revised form January 10, 2006)

The main goal of this work was to evaluate the effectiveness of Walker's equation in collapsing the fatigue crack propagation data of a SAE AMS 7475-T7351 aluminum alloy loaded either longitudinally (L-T) or transversely (T-L) to the rolling direction. T-L orientation testpieces presented lower ductility and fracture toughness values than L-T orientation. As a consequence, during the fatigue crack propagation tests, T-L testpieces exhibited a stronger influence of monotonic modes of fracture, resulting in higher Paris exponent values, *m*. Walker's model was able to collapse fatigue crack propagation data of L-T test pieces at different applied stress ratios, *R*. However, for the T-L orientation, due to the *R* ratio dependency on *m* and *C*, simply averaging of *m* values for the calculations of Walker's exponent proved to be inefficient. A simple analytical procedure was proposed by the authors to modify Walker's model to take into account such effect. For T-L test pieces, when Walker's model is modified by considering both Paris's exponent as well the coefficient as a function of the *R* ratio, the fatigue crack growth data collapses within a narrow band, thus allowing predictions to be made satisfactorily. The collapsed band is even narrower if the empirical relation $m = a+b\log C$ is used instead of simple polynomial equations due to a better correlation coefficient.

Keywords aluminum alloy, fatigue crack propagation, *R* ratio, Walker's model

1. Introduction

Aluminum alloys are widely used in the aerospace industry due to their high specific strength. In particular, the 7xxx series has been used for structural applications, such as airframes. During flight operation, the aircraft is subjected to variable amplitude loading conditions, which in other words means that when a crack is present, the material experiences a wide range of stress intensity factor ranges (ΔK) and stress ratios (R). To make accurate life predictions, equations taking into account R ratio effects on the fatigue crack propagation rate (da/dN) must be used. Over the past 40 years, several researchers have attempted to model the fatigue crack growth behavior of materials to take into account the R ratio effect by using either empirical, physical, or closure approaches (Ref 1–10). In particular, Walker (Ref 11) proposed an empirical relation where an effective stress, $\overline{S}$, is capable of predicting the effect of R ratio on da/dN:

$$\overline{\Delta S} = (1 - R)^{-(1-w)}\,\Delta S \qquad \text{(Eq 1)}$$

where ΔS is the applied stress range, w is the Walker exponent that is assumed to be a material constant dependent on the R ratio. This equation can be rewritten in terms of an effective stress intensity factor range, $\overline{\Delta K}$:

E. Di Todaro, C.T.O.F. Ruckert, M.T. Milan, W.W. Bose Filho, J.R. Tarpani, and **D. Spinelli**, NEMAF - Núcleo de Ensaios de Materiais e Análises de Falhas, Departamento de Engenharia de Materiais, Aeronáutica e Automobilística, Escola de Engenharia de São Carlos – Universidade de São Paulo, CEP: 13566-590, São Carlos, SP, Brazil. Contact e-mails: cassius@sc.usp.br and mtmilan@sc.usp.br.

$$\overline{\Delta K} = (1 - R)^{-(1-w)}\,\Delta K \qquad \text{(Eq 2)}$$

It is important to note that if $R = 0$, then, $\overline{\Delta K}$ (i.e., Walker's equation collapses the fatigue crack growth data at $R = 0$). Then, the Paris-Erdogan equation can be modified accordingly:

$$\frac{da}{dN} = C_0\,(\overline{\Delta K})^{m_0} = C_0(1 - R)^{-(1-w)m_0}\,(\Delta K)^{m_0} \qquad \text{(Eq 3)}$$

List of Symbols

C	Paris coefficient
C_0	Paris coefficient for $R = 0$
da/dN	crack growth rate
K	applied stress intensity factor
K_{max}	maximum applied stress intensity factor
$K_Q(5\%)$	provisional fracture toughness measured by the 5% tangent drop method
K_{IC}	mode I plane strain fracture toughness
m	Paris exponent
m_0	Paris exponent for $R = 0$
R	applied stress ratio
r^2	coefficient of correlation
RA	area reduction
S	applied stress
S_{ys}	0.2% offset yield stress
UTS	ultimate tensile strength
w	Walker's exponent
ΔK	applied stress intensity factor range
$\overline{\Delta K}$	Walker's effective stress intensity factor range
ΔS	applied stress range
$\overline{\Delta S}$	Walker's effective stress range
ε_t	total elongation to failure

Table 1 Chemical analysis results (wt.%)

Zn	Mg	Cu	Cr	Fe	Si	Ti	Al
5.79	1.95	1.76	0.24	0.07	0.05	0.05	Balance

where C_0 and m_0 are the Paris coefficient and exponent respectively, noting that $C_0 = C_{R=0}$ and $m_0 = m_{R=0}$.

According to Rosenfeld (Ref 12), Eq 1 to 3 can be applied in cases where the fatigue crack growth lines are parallel. Consequently the Paris exponent m is constant regardless of the R ratio. In the analytical procedure proposed by Zheng and Powell (Ref 13), small differences in m are considered by averaging the values at the different R ratios. Therefore, the term $C_0 (1 - R)^{-(1-w)m_0}$ in Eq 3 is the Paris coefficient, C, for a specific R ratio:

$$C = C_0(1 - R)^{-(1-w)m_0} \quad \text{(Eq 4)}$$

Applying logarithmic transformation on both sides:

$$\log C = \log C_0 - (1 - w)m_0 \log(1 - R) \quad \text{(Eq 5)}$$

where $\log C_0$ and $-(1\text{-}w)m_0$ are the equation coefficients that are obtained through linear regression analysis of the log$C$ versus log$(1\text{-}R)$ plot, thus allowing w to be calculated.

The main purpose of this work was to evaluate the effectiveness of Walker's approach in collapsing *da/dN* data of a SAE AMS 7475-T7351 aluminum alloy loaded either longitudinally (L-T) or transversely (T-L) to the rolling direction. Depending on the loading direction, the material shows a different behavior for the fracture toughness and its effect on Walker's approach can be assessed.

2. Experimental Procedures

The material of this study was supplied by EMBRAER–Brazil and consists of a 60 mm thick plate of 7475-T7351 aluminum alloy. The chemical composition given in Table 1 shows that the values are within those specified by SAE AMS 2355 standard (Ref 14).

C(T) test pieces for fracture toughness and fatigue crack propagation tests were machined by electro-discharge machining in two different orientations, as depicted schematically in Fig. 1. For the fracture toughness tests, a fatigue precrack was introduced. The final maximum applied stress intensity factor during precracking was less than 60% of the estimated K_{IC} of the material. The fracture toughness tests were performed in accordance to ASTM E1820-01 (Ref 15), in air, at room temperature in both orientations (L-T, T-L). Tensile tests were also performed in both orientations, in air at room temperature, at a crosshead speed of 5 mm/min according to ASTM E8M-00 (Ref 16). Fatigue crack growth tests were performed according to ASTM E647-00 (Ref 17), in air, at room temperature, under constant load range, R ratios of 0.1, 0.5, 0.7, and 0.8 at frequency of ~15 Hz. Fatigue test pieces were also tested in both orientations. The crack growth was monitored using the compliance technique.

3. Results and Discussion

3.1 Monotonic Properties

Tensile and fracture toughness results and the corresponding standard deviation values (δ) are presented in Table 2. The results are the average values of four tests. For all fracture toughness test pieces, provisional K_Q conforms to the validity conditions for the plane strain fracture toughness K_{IC}, as given by ASTM 1820-01 (Ref 15). The investigated 7475-T7351 aluminum alloy presented similar strength values in both orientations studied.

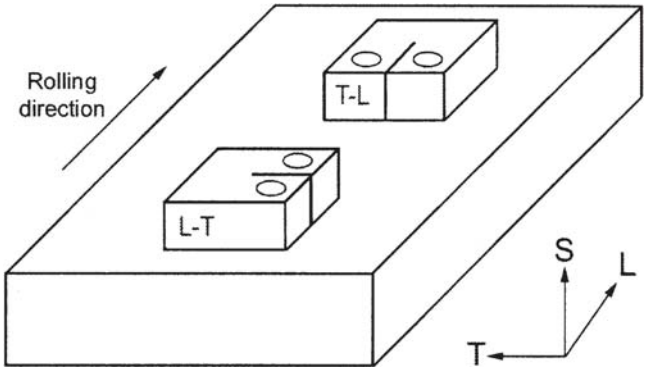

Fig. 1 Schematic representation of testpiece orientation used in fracture toughness and fatigue crack propagation tests.

Table 2 Tensile and fracture toughness results

Orientation	UTS, MPa	S_{ys}, MPa	RA, %	ε_t, %	K_{IC}, MPa.m$^{1/2}$
L-T	469 (13.3)	395 (13.0)	19 (3.4)	16 (1.2)	50.5 (0.9)
T-L	472 (12.3)	398 (10.9)	15 (0.8)	11 (0.5)	37.1 (0.4)

Note: The numbers in parenthesis refer to δ values. UTS, ultimate tensile strength

However, when ductility and fracture toughness values are simultaneously analyzed, a different picture emerges. For T-L orientation, where the fracture takes place along the rolling direction, on the SL plane (as observed in Fig. 1), a distinguished reduction in both ductility and fracture toughness values was observed. Micrographic analysis showed that the ST plane presented randomly distributed particles within the microstructure, while the SL plane (Fig. 2) presented clustered second phase particles aligned with the rolling direction, which is likely to favor a reduction of ductility values for test pieces tested in the T-L orientation, by creating a weaker path for crack growth. Several studies have shown that particle clustering contribute to the failure process by imposing high levels of plastic constraint to the matrix adjacent to the particles, raising stress triaxiality to a level significantly higher than that normally associated with matrix failure (Ref 18–20) providing favorable paths for linkage of damage ahead of the crack tip (Ref 21). Additionally, when the crack grows along the rolling direction, it traverses a smaller number of grain boundaries, spending less specific energy for crack growth.

3.2 Stress Ratio and Test Piece Orientation Effects

Before analyzing the efficiency of Walker's approach in collapsing the fatigue data of the present work, it is convenient to analyze first the effects of both stress ratio and test piece orientation on the fatigue crack growth resistance of 7475-T7351 aluminum alloy.

Figure 3 depicts the effects of different R ratios applied during the fatigue crack growth tests performed in the 7475-

T7351 aluminum alloy. In L-T orientation (Fig. 3a), there was little difference in *da/dN* values within the Paris region. Additionally, the Paris exponent, *m*, remains nearly constant for all *R* ratios imposed to the tests, as observed in Table 2. However, in T-L orientation (Fig. 3b), considering the same applied ΔK, *da/dN* values diverge steeply when the different *R* ratio curves are compared. Assuming that closure levels are similar for both orientations, it is suggested that this result is due to the fact that the T-L orientation testpieces are likely to be more affected by the contribution of monotonic modes of fracture because the material exhibited lower toughness values in this orientation, as discussed previously. Indeed, *m* values for T-L test pieces are higher than those obtained for the L-T orientation increased significantly as the *R* ratio increases (Table 3), giving support to the idea of a stronger K_{max} dependence.

Direct comparisons between L-T and T-L orientation testpieces, tested at different *R* ratios, are presented in Fig. 4. It was observed that for the *R* ratio of 0.1 (Fig. 4a), the effect of testpiece orientation on *da/dN* values is not significant in the Paris region. However, for higher applied *R* ratios (Fig. 4b-d), testpieces tested in the T-L orientation presented higher *da/dN* values for intermediate to high applied ΔK levels. Again, these results can be rationalized by the fact that the T-L orientation testpieces presented inherently lower toughness leading to higher slopes in the Paris region, i.e., higher *m* values.

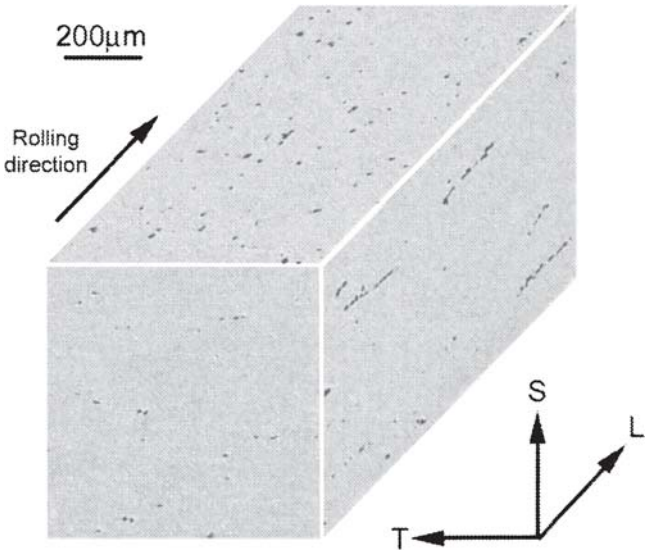

Fig. 2 Micrographic analysis of second phase particles

3.3 Walker's Model

Figure 5(a) shows the result of Walker's model applied to the fatigue crack growth data of L-T orientation testpieces. It is observed that the curves collapsed into a narrow band and consequently the model was suitable to predict *da/dN* values for any given *R* ratio in this orientation. On the other hand, when Walker's model was applied to the T-L orientation testpieces, instead of collapsing the data into a narrow band equivalent to $R = 0$ curve, the data shifted apart, moving to the left hand side of the graph, as depicted in Fig. 5(b).

These results clearly demonstrate the unsuitability of Walker's model in describing the *R* ratio effects when *m* values are not constant. The Paris exponent used in *w* calculations was assumed to be an average of *m* values for different *R* ratios, as proposed by Zheng et al. (Ref 13). However, it was seen that *m* values are dependent on *R* for T-L test pieces. Therefore a simple modification to Walker's model is proposed below, which incorporates the *R* dependence on *m.*

For a specific value of *R*, the fatigue crack growth rate, *da/dN,* can be given by the well-known Paris-Erdogan equation:

$$\frac{da}{dN} = C(\Delta K)^m \quad \text{(Eq 6)}$$

Combining Eq 3 with Eq 6 yields:

$$C(\Delta K)^m = C_0\,(1-R)^{-(1-w)m_0}\,(\Delta K)^{m_0} \quad \text{(Eq 7)}$$

If the fatigue crack propagation curves at different *R* ratios are parallel (i.e., *m* is independent of the *R* ratio), then $m = m_0$. The Eq 7 simplifies back to Eq 4.

Rearranging Eq 7:

$$(1-R)^{-(1-w)m_0} = \frac{C}{C_0}\,(\Delta K)^{m-m_0} \quad \text{(Eq 8)}$$

Applying logarithmic transformation on both sides:

$$-(1-w)m_0 \log(1-R) = \log C - \log C_0 + (m-m_0)\log(\Delta K) \quad \text{(Eq 9)}$$

Finally, Walker's exponent can be written as:

$$w = 1 + \frac{\log C - \log C_0 + (m-m_0)\log(\Delta K)}{m_0 \log(1-R)} \quad \text{(Eq 10)}$$

Equation 10 indicates that Walker's exponent is no longer a simple material constant, but it depends on both the *R* ratio and ΔK levels. This requires the knowledge of C_0, m_0, and $m = f(R)$

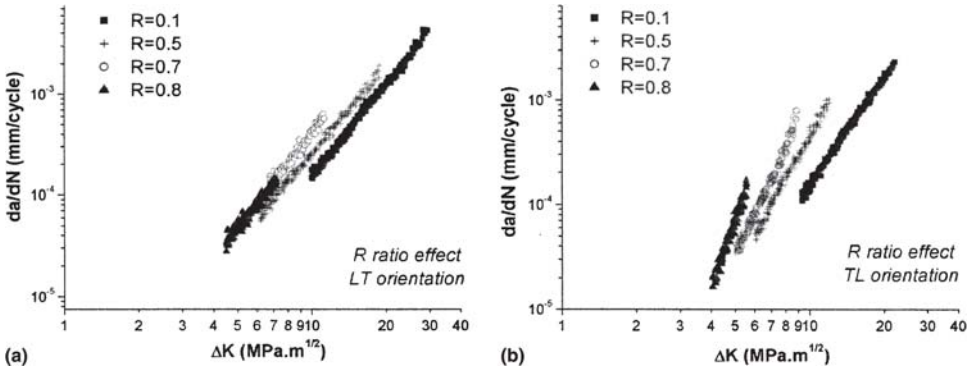

Fig. 3 *R* ratio effects on *da/dN* values for SAE AMS 7475-T7351 aluminum alloy: (a) L-T orientation and (b) T-L orientation

Table 3 Paris coefficient and exponent for T-L and L-T test piece orientations

Orientation	Parameter	$R = 0.1$	$R = 0.5$	$R = 0.7$	$R = 0.8$
L-T	m	3.02	2.90	3.00	2.93
	C (mm/cycle)	1.43×10^{-7}	3.17×10^{-7}	3.98×10^{-7}	4.21×10^{-7}
T-L	m	3.47	4.33	5.01	6.30
	C (mm/cycle)	5.10×10^{-8}	2.14×10^{-8}	1.02×10^{-8}	2.73×10^{-9}

Note: L-T, longitudinally to the rolling direction; T-L, transversely to the rolling direction

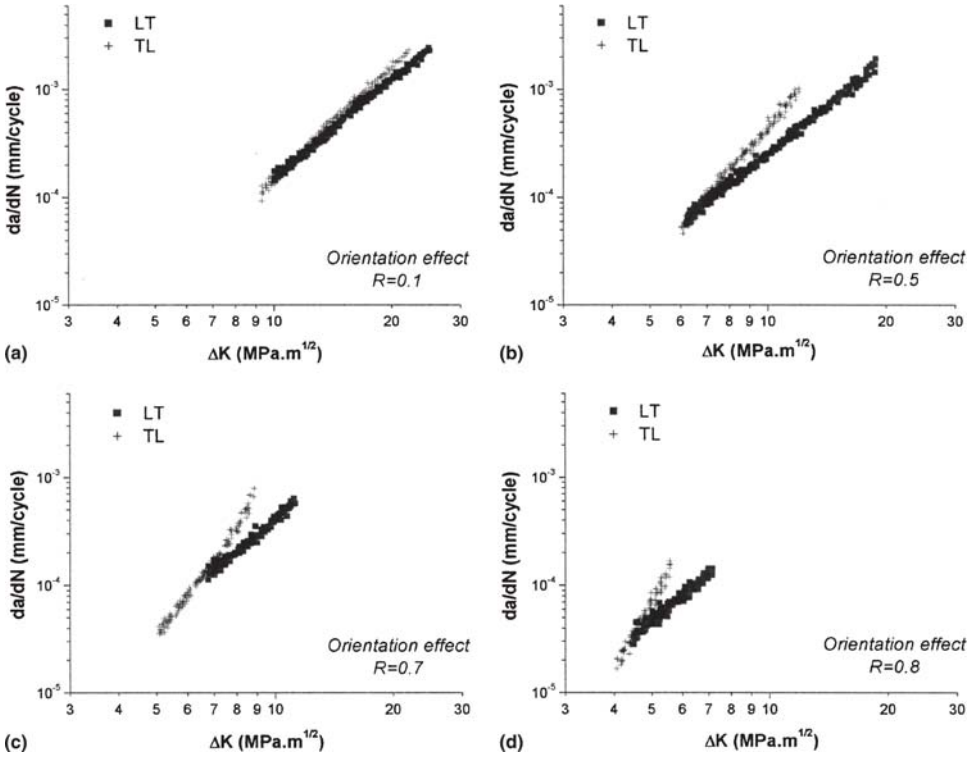

Fig. 4 Test piece orientation effects on *da/dN* values of SAE AMS 7475-T7351 aluminum alloy: (a) $R = 0.1$, (b) $R = 0.5$, (c) $R = 0.7$ and (d) $R = 0.8$

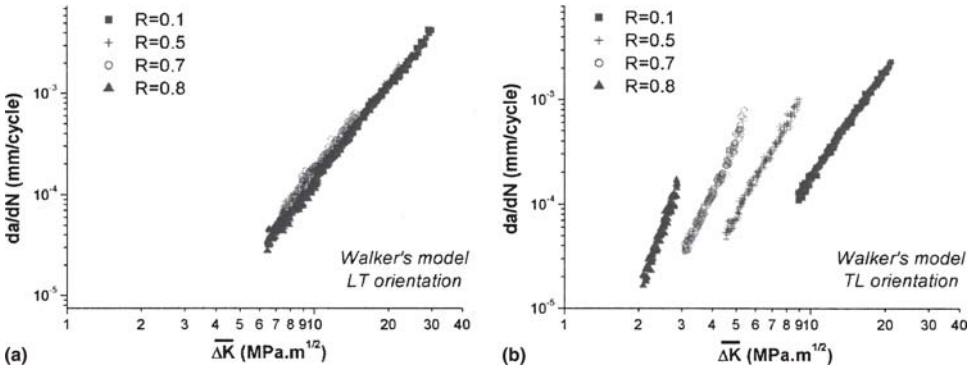

Fig. 5 Walker's model applied to fatigue crack growth data: (a) L-T orientation and (b) T-L orientation

to be calculated. As a first approach, these can be obtained through simple regression analyses of curve plotted in the polynomial function. The obtained results for the present alloy are presented in Fig. 6. The constant C was found to be very well correlated to the R ratio by a parabolic equation, as seen in Fig. 6(a). Two different polynomial equations were used to adjust m values, as seen in Fig. 6(b). It was observed that the second-degree polynomial presented the best correlation coefficient.

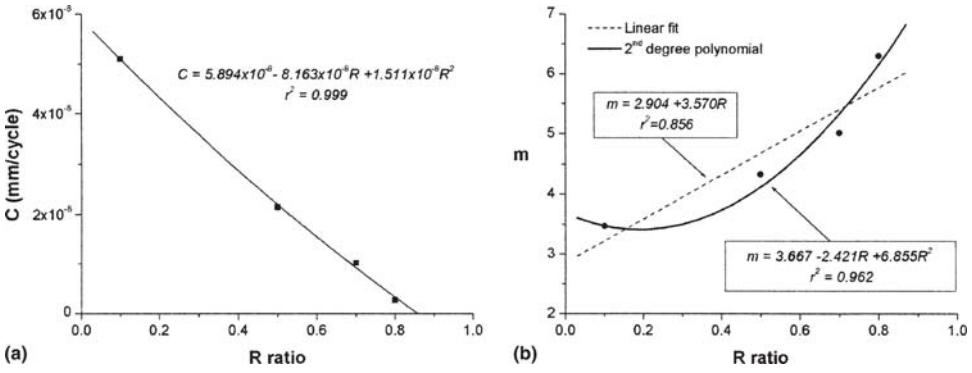

Fig. 6 Dependence of (a) C and (b) m, on R for T-L orientation test pieces

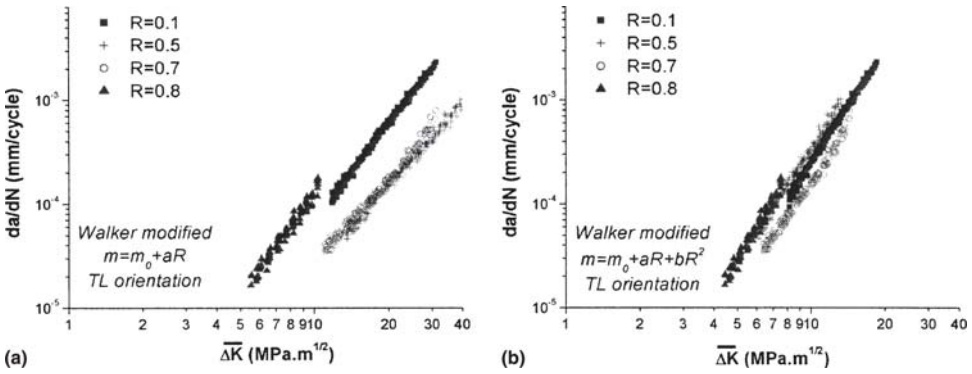

Fig. 7 Results of Walker's model modified to take into account R ratio effects on m values: (a) using a linear fit ($m = m_0+aR$) and (b) using a second-degree polynomial ($m = m_0+aR+bR^2$).

When the linear fit equation presented in Fig. 6(b) is used in Eq 10, a significant improvement in Walker's model was obtained. As depicted in Fig. 7(a), the curves approached to each other, towards the $R = 0$ curve. However, as seen in Fig. 7(b), a further improvement was obtained when m was correlated to R by a second-degree polynomial, which exhibits a higher correlation coefficient than the linear fit. In this case, the curves obtained at different R ratios collapsed within a narrower band.

Although the use of a polynomial function to describe m as a function of R resulted in an improvement in Walker's model, the data is not perfectly collapsed. In this sense, a different approach was used to describe m as a dependent variable on R. Previous work (Ref 22) has shown that m and C can be correlated by the following empirical relationship:

$$m = a + b \log C \qquad \text{(Eq 11)}$$

where a and b can be obtained through regression analysis of the m versus log$C$ plot.

In this case, the effect of R on m is taken into account indirectly by the Paris coefficient. Therefore, if m, as given in Eq 11, is placed in Eq 10, the following equation for Walker's exponent is obtained:

$$w = 1 + \frac{(\log C - \log C_0)(1 + b)\log(\Delta K)}{(a + b \log C_0)\log(1 - R)} \qquad \text{(Eq 12)}$$

Figure 8 shows m-log$C$ plot for the material of the present work. One can observe that an excellent correlation coefficient was obtained. Consequently, when Eq 12 is used to calculate w of Walker's model, the fatigue crack propagation data of the T-L orientation testpieces collapsed into a perfectly narrow band, as depicted in Fig. 9, thus allowing predictions to be made with a larger degree of precision than the previous attempts. The results presented in Fig. 7 and 9 suggest that the success in collapsing the fatigue crack growth data of K_{max} dependent materials into a narrow band, strongly depends on the correct choice of the equation describing the relationship between C, m, and R. When a simple average of m values is considered (Fig. 5b), the correlation is very poor and the model simply does not work. As the correlation factor increases, the model improves significantly. It is important to emphasize that these results are limited to the data of the present work although the Eq 12 is analytically consistent, it depends on empirical relationships. Therefore, its general applicability must be tested in other materials whose C and m values are dependent on R.

4. Conclusions

The following conclusions can be drawn in relation to the SAE AMS 7475-T7351 aluminum alloy:

1) T-L orientation test pieces presented lower ductility as well as fracture toughness values than the L-T orientation. This was attributed to the precipitation of second phase particles aligned with the rolling direction, which creates a weaker

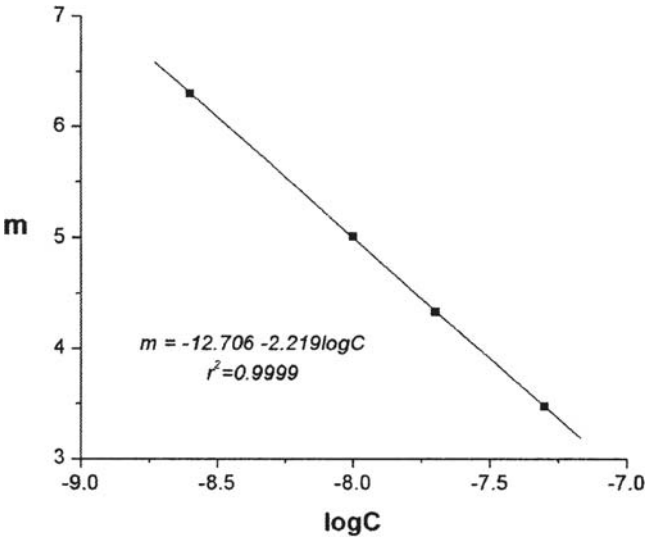

Fig. 8 *m*-log*C* plot for T-L orientation testpieces

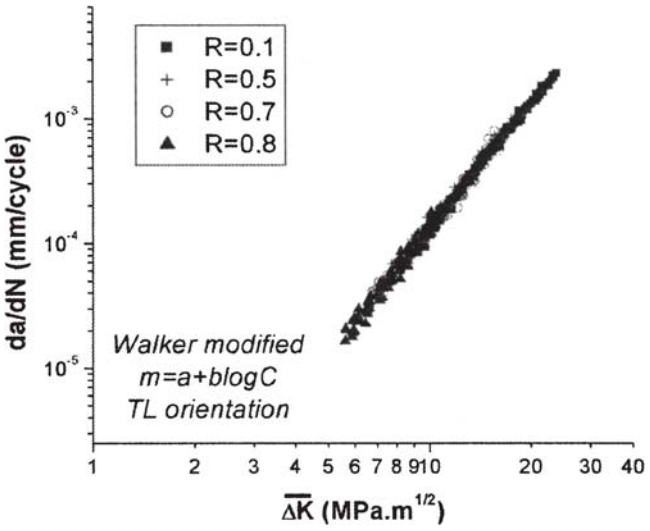

Fig. 9 Results of Walker's model modified using $m = a+b\log C$ and applied to fatigue crack growth data of T-L orientation test pieces

path for crack growth. Additionally, the crack must traverse a smaller number of grain boundaries along the fracture plane, spending less specific energy for cracking. As a consequence, during the fatigue crack propagation tests, T-L testpieces exhibited a stronger K_{max} dependence, resulting in higher m values within the Paris region.

2) Walker's model is able to collapse fatigue crack propagation data of L-T test pieces at different R ratios. However, for the T-L orientation, due to the R dependency on m, the simple approach of averaging m values for the calculations of Walker's exponent proved to be inefficient.
3) For T-L testpieces, when Walker's model is modified by considering both C and m as functions of the R ratio, the fatigue crack growth data collapses within a narrow band, thus allowing predictions to be made satisfactorily. The collapsed band is even narrower if the empirical relation $m = a+b\log C$ is used instead of simple polynomial equations due to a better correlation coefficient. Therefore, the success in collapsing the fatigue data proved to be strongly dependent on the correct choice of the function describing the association of m, C, and R ratio.

Acknowledgments

The authors thank FAPESP-Brazil for providing the financial support of this work (Grants: 99/01042-0, 02/09027-4) and EMBRAER-Brazil for providing the materials used in this research.

References

1. R.G. Forman, V.E. Keary, and R.M. Engle, Numerical Analysis of Crack Propagation in Cyclic-Loaded Structures, *J. Basic Eng.,* 1967, **89,** p 459-464
2. J. Weertman, Rate of Growth of Fatigue Cracks Calculated from the Theory of Infinitesimal Dislocations Distributed on a Plane, *Int. J. Fract. Mech.,* 1966, 2460-2467
3. M. Klesnil and P. Lukas, Influence of Strength and Stress History on Growth and Stabilization of Fatigues Cracks, *Eng. Fract. Mech.,* 1972, **4,** p 77-92
4. R.J. Donahue, H.M. Clark, P. Atanmo, R. Kumble, and A.J. McEvily, Crack Opening Displacement and the Rate of Fatigue Crack Growth, *Int. J. Fract. Mech.,* 1972, **8,** p 209-219
5. A.J. McEvily, On Closure in Fatigue Crack Growth, *Mechanics of Fatigue Crack Closure,* ASTM STP 982, 1988, p 35-43
6. A.K. Vasudevan, K. Sadananda, and N. Louat, A Review of Crack Closure, Fatigue Crack Threshold and Related Phenomena, *Mater. Sci. Eng. A,* 1994, **188A,** p 1-22
7. A.J. McEvily and R.O. Ritchie, Crack Closure and Fatigue Crack Propagation Threshold as a Function of Load Ratio, *Fat. Fract. Eng. Mater. Struct.,* 1998, **21,** p 847-855
8. D. Kujawski, A New $(\Delta K+K_{max})0.5$ Driving Force Parameter for Crack Growth in Aluminum Alloys, *Int. J. Fat.,* 2001, **23,** p 733-740
9. D. Kujawski, Enhanced Model of Partial Crack Closure for Correlation of R-ratio Effects in Aluminum Alloys, *Int. J. Fat.,* 2001, **23,** p 95-102
10. W.T. Riddel and R.S. Piascik, Stress Ratio Effects on Crack Opening Loads and Crack Growth Rates in Al Alloy 2024, *NASA,* 1998, **TM-206929,** p 1-17
11. K. Walker, The Effect of Stress Ratio During Crack Propagation and Fatigue for 2024-T3 and 7075-T6 Aluminum, *Effects of Environment and Complex Load History on Fatigue Life,* ASTM STP462, 1970, p 1–14
12. A.R. Rosenfeld, Fracture Mechanics in Failure Analysis, *Metals Handbook: Fatigue and Fracture,* 10th ed., vol. 19, ASM International, 1997, p 450-456
13. J. Zheng and B.E. Powell, Effect of Stress Ratio and Test Methods on Fatigue Crack Growth Rate for Nickel Based Superalloy Udimet720, *Int. J. Fat.,* 1999, **21**(5), p 507-513
14. SAE AMS 2355, Quality Assurance Sampling and Testing of Aluminum Alloys and Magnesium Alloys, *Wrought Products, Except Forging Stock, and Rolled, Forged, Or Flash Welded Rings, Aer. Mat. Spec.,* SAE Int., 2002
15. "Standard Test Method for Measurement of Fracture Toughness. American Society for Testing and Materials," E1820-01, *Annual Book of ASTM Standards,* vol.03.01, ASTM, 2001
16. "Standard Test Methods for Tension Testing of Metallic Materials [Metric]. American Society for Testing and Materials," E8M-00, *Annual Book of ASTM Standards,* vol.03.01, ASTM, 2000
17. "Standard Test Method for Measurement of Fatigue Crack Growth Rates. American Society for Testing and Materials," E647-00, *Annual Book of ASTM Standards,* vol.03.01, ASTM, 2000
18. C. Cui, R. Wu, Y. Li, and Y. Shen, Fracture Toughness of In Situ TiCp-AlNp/AL Composite, *J. Mater. Proc. Tech.,* 2000, **100,** p 36-41
19. W.H. Hunt, T. Osman, and J.J. Lewandowski, Micro and Macrostructural Factors in DRA Fracture Resistance, *J. Mater.,* 1993, **45**(1), p 30-35
20. I.C. Stone and P. Tsakiropoulos, The Effect of Reinforcement on the Notched and Unnotched Room Temperature Tensile Properties of AL-4wt.%Cu:SiC MMCs, *Mater. Sci. Eng. A,* 1998, **A241,** p 19-29
21. C.P. You, A.W. Thompson, and I.M. Bernstein, Aging Effects on Fatigue Crack Growth and Closure in a SiC Reinforced 2124 Aluminum Composite, *J. Metall.,* 1988, **40**(7), p A88
22. E.H. Niccolls, A Correlation for Fatigue Crack Growth Rate. *Scripta Metall. Scripta Metall.,* 1976, **10,** p 295-298